Developmental Cell
Article

Arabidopsis Regeneration from Multiple Tissues Occurs via a Root Development Pathway

Kaoru Sugimoto,[1] Yuling Jiao,[1] and Elliot M. Meyerowitz[1,*]
[1]Division of Biology 156-29, California Institute of Technology, Pasadena, CA 91125, USA
*Correspondence: meyerow@its.caltech.edu
DOI 10.1016/j.devcel.2010.02.004

SUMMARY

Unlike most animal cells, plant cells can easily regenerate new tissues from a wide variety of organs when properly cultured. The common elements that provide varied plant cells with their remarkable regeneration ability are still largely unknown. Here we describe the initial process of *Arabidopsis* in vitro regeneration, where a pluripotent cell mass termed callus is induced. We demonstrate that callus resembles the tip of a root meristem, even if it is derived from aerial organs such as petals, which clearly shows that callus formation is not a simple reprogramming process backward to an undifferentiated state as widely believed. Furthermore, callus formation in roots, cotyledons, and petals is blocked in mutant plants incapable of lateral root initiation. It thus appears that the ectopic activation of a lateral root development program is a common mechanism in callus formation from multiple organs.

INTRODUCTION

All cell types that compose multicellular organisms are derived from a single totipotent cell, the fertilized egg, through successive cell division and differentiation processes. In animals, most cells lose their range of differentiation ability as they are specified and differentiate into specific cell types, except for stem cells. On the contrary, plant cells have been thought to maintain totipotency, because they are competent to regenerate the full array of plant tissues from already differentiated organs (Birnbaum and Sanchez Alvarado, 2008; Skoog and Miller, 1957). A wide variety of plant tissues has been shown to regenerate whole plants under proper culture conditions (Halperin, 1986; Skoog and Miller, 1957). However, the mechanisms behind the totipotency of plant cells still remain elusive (Birnbaum and Sanchez Alvarado, 2008; Vogel, 2005).

The developmental fate of regenerating tissue can be directed by the ratio of two plant hormones, auxin and cytokinin (Skoog and Miller, 1957). With these hormones, a huge number of culture conditions have been tested in various species of plant tissues. In *Arabidopsis*, one of the most commonly used in vitro regeneration systems was developed by Valvekens et al. (1988) (Weigel and Glazebrook, 2002). In this system, small pieces of plant tissue (explants) are sequentially subjected to two hormonal treatments. In the first step, a mass of growing cells (callus) is formed from explants on auxin-rich callus-inducing medium (CIM). Subsequent culture of the callus on shoot- or root-inducing medium containing different ratios of auxin to cytokinin causes the cells to be specified and differentiate into shoot or root tissues (Figure S1 available online). Cells are thought to dedifferentiate and acquire competency when they divide to form callus (Gautheret, 1966). Another possibility is that some kind of pre-existing cell, like a stem cell, within an explant might selectively proliferate and form callus. Because of its high regeneration ability and unorganized surface structure, callus has long been believed to be undifferentiated tissue. But it is only recently that the actual differentiation state of callus-forming cells has started to be described at a molecular level. Atta et al. have recently shown that callus derived from root and hypocotyl explants has many characteristics of lateral root meristem (Atta et al., 2008).

Lateral root formation starts with a series of divisions of pericycle cells, a layer of root tissue surrounding the vasculature (Kurup et al., 2005; Malamy and Benfey, 1997). A limited number of pericycle cells, associated with the two xylem poles of the primary root, undergoes ordered cell divisions and differentiation, leading to a multilayered structure. Further periclinal divisions of the cells produce all of the cell layers present in a root and form a lateral root primordium (LRP), which resembles the primary root tip. Finally, the LRP grows and emerges outside the primary root. After emergence, a functional lateral root apical meristem is activated and the lateral root continues growing (Malamy and Benfey, 1997).

Similarly to lateral root initiation, callus formation from root and hypocotyl explants initiates with divisions of pericycle cells, and expression of a few root apical meristem markers is observed in the resulting callus tissue (Atta et al., 2008; Che et al., 2007; Laplaze et al., 2005). Both roots and hypocotyls are basal tissues derived from the basal half of embryo, which are widely used as a tissue source for the *Arabidopsis* regeneration assay. Although various types of plant tissues including aerial organs have been shown to form callus, it remains unknown whether callus derived from different tissues is equivalent in its differentiation state and whether common processes drive regeneration from different tissues (Birnbaum and Sanchez Alvarado, 2008).

Here we show that callus derived from aerial organs, such as petals and cotyledons, also resembles the tip of a root meristem. Moreover, our mutant analysis and observation of pericycle marker expression in root, cotyledon, and petal explants suggest that the ectopic activation of a lateral root initiation program from cells equivalent to root pericycle cells is the common mechanism of callus formation from these organs. Thus, the differentiation of

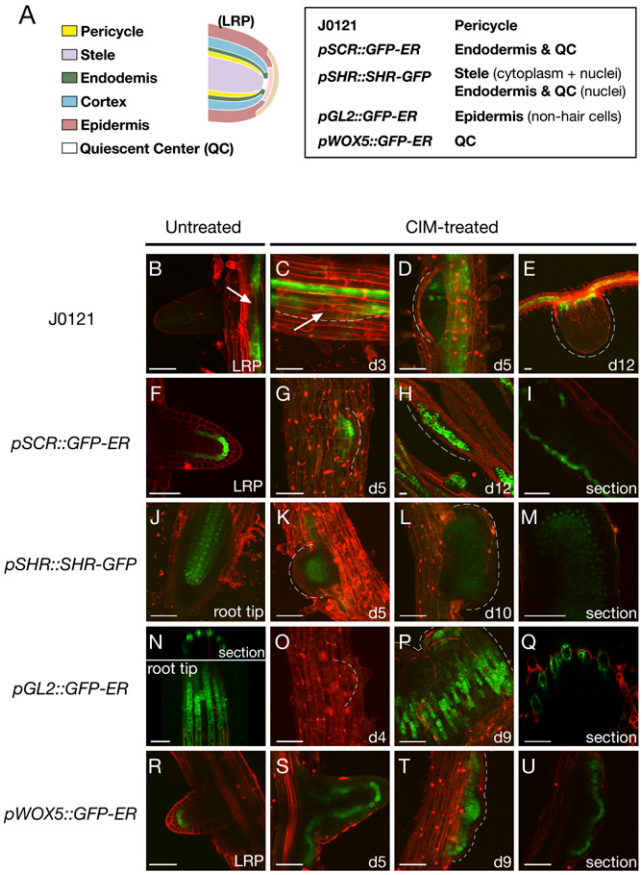

Figure 1. Callus Derived from Root Is a Moderately Organized Tissue Similar to a Lateral Root Primordium

(A) Schematic diagram of lateral root primordium (LRP) and the root tissue markers used.

(B–U) The markers expression (green) in root explants before (left column) and after (right three columns) CIM treatment. The number of days of CIM incubation is indicated at the bottom right corner of each panel. The panels (I), (M), (Q), and (U) are single optical sections, and all the other panels are projections from confocal z-stacks. Cellular outlines were visualized with propidium iodide staining (red). White dotted lines indicate callus-forming regions. The growing regions in (C), (G), and (O) were outlined according to the single optical section views. J0121 (B)–(E), *pSCR::GFP-ER* (F)–(I), *pSHR::SHR-GFP* (J)–(M), *pGL2::GFP-ER* (N)–(Q), and *pWOX5::GFP-ER* (R)–(U). The arrows in (B) and (C) indicate the disappearance of the marker signal. Scale bars represent 50 μm. See also Figure S1.

pericycle-like cells toward a root meristem-like tissue is a process shared in the formation of callus from multiple organs.

RESULTS

Callus Derived from Root Is an Organized Tissue Similar to LRP

To further investigate the organization of root callus as compared to the forming lateral root (Atta et al., 2008; Che et al., 2007), and to obtain basic information on callus derived from aerial organs, we used live imaging to follow the expression pattern of cell type markers that are expressed in LRP (Figure 1A). We first examined the expression of J0121, a marker for the twin files of pericycle cells associated with xylem poles of the vasculature, that divide to give rise to LRP (Laplaze et al., 2005). Callus formation from root explants has been shown to start with a series of divisions of pericycle cells (Atta et al., 2008; Che et al., 2007). As reported previously (Che et al., 2007; Laplaze et al., 2005), the J0121 signal was diffuse in the broad growing region upon callus induction on CIM, as is observed at the base of LRP in untreated explants (Figures 1B–1D), indicating a fate change of pericycle cells. The signal was eventually localized at the base of the mature callus and the expression level remained strong through all stages afterward (Figure 1E). Second, we examined *pSCR::GFP-ER*, a marker for endodermis and quiescent center (QC) cells (Figure 1F; Wysocka-Diller et al., 2000), and *pSHR::SHR-GFP*, a marker for the cytosol and nuclei of stele cells and nuclei of surrounding endodermal and QC cells (Figure 1J; Nakajima et al., 2001). The signals in both marker lines were confined to the callus-forming region until day 4 on CIM (Figures 1G, 1H, 1K, and 1L). As in roots, *pSCR::GFP-ER* expression was confined to subepidermal layers throughout the callus region (Figure 1I). *pSHR::SHR-GFP* expression also mirrored the pattern in LRP in that nuclear-localized expression indicative of the endodermis and QC was observed in the outer subepidermal cell layers, and stele-like localization patterns were internal to that (Figure 1M). A third marker for non-hair epidermal cells in the meristematic zone of primary root and LRP, *pGL2::GFP-ER* (Figure 1N; Lin and Schiefelbein, 2001), initially lost expression from whole explants, and then the expression gradually recurred in callus from day 7 to day 9 on CIM (Figures 1O and 1P). Expression was in a striped pattern in the callus epidermis, as in roots (Figures 1P and 1Q). Therefore, in this assay, root callus maintains a layered radial organization similar to that of LRP (Figures 1I, 1M, and 1Q). All of these data together indicate that callus is not an undifferentiated cell population but a differentiated tissue similar to LRP, which confirms and extends the conclusions of Atta et al. (2008).

Callus Resembles the Tip Part of the Root Meristem

A pronounced difference between root callus and LRP was that *pWOX5::GFP-ER*, a reporter specific to QC cells in the tip of LRP (Figure 1R; Blilou et al., 2005), was expressed throughout the subepidermal layer of the whole callus (Figures 1T and 1U). During 2–5 days on CIM, the marker expression spread from QC cells to the surrounding endodermal cells (Figure 1S). Finally, expression appeared to coincide with *pSCR::GFP-ER* expression (Figures 1H, 1I, 1T, and 1U). QC cells are the mitotically inactive organizing center of the root stem cell niche and are found at the auxin maximum (Grieneisen et al., 2007). CIM contains the nontransportable auxin analog 2,4-D, which disrupts the auxin gradient of the root (Geldner et al., 2004). Taking into consideration that all *SCR*-expressing endodermal cells are suggested to be competent to acquire QC identity depending upon the auxin distribution (Sabatini et al., 2003), we hypothesized that broad *WOX5* reporter expression in callus might be caused by the impaired auxin gradient. To confirm this, we compared the effects of CIM containing the transportable auxin analog NAA with the original CIM containing nontransportable 2,4-D on *WOX5* and *SCR* reporter expression patterns in explants. *pWOX5::GFP-ER* signal was detected only in the tip of LRP at a low concentration of NAA (Figure 2B), whereas 2,4-D or a high concentration of NAA, such that the whole root

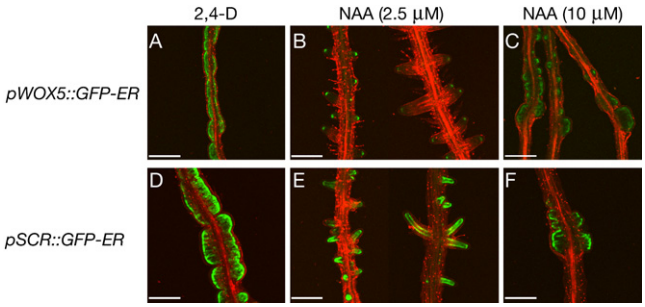

Figure 2. Callus Resembles the Tip Part of the Lateral Root Meristem

pWOX5::GFP-ER (A)–(C) and *pSCR::GFP-ER* (D)–(F) marker expression (green) in the root explants treated for 10 days with NAA or 2,4-D. (A) and (D) 2,4-D (same concentration as normal CIM); (B) and (E) 2.5 μM NAA; (C) and (F) 10 μM NAA. Cellular outlines were visualized with propidium iodide staining (red). Scale bars represent 50 μm.

achieved high auxin levels, caused broad expression (Figures 2A and 2C). The *pSCR::GFP-ER* reporter showed broad expression in the endodermal layer in every condition (Figures 2D–2F). Therefore, *SCR* reporter expression in callus represents QC-like cells, and the entire callus formed in 2,4-D CIM resembles the tip part of LRP as it appears near the auxin maximum in the nontreated wild-type root.

Callus Derived from Aerial Organs Shows LRP-like Structure, just as Callus Derived from Roots

We next made callus from aerial organs and observed reporter expression, to investigate what properties are shared among callus tissues of different origin. We picked cotyledons and petals as the source for callus induction because each of these organs is distinct from the others and from roots in their position, developmental origin, and cell types. Cotyledons and petals are derived from the apical half of embryo, unlike the roots and hypocotyls. Primary roots and cotyledons are of embryonic origin, whereas lateral roots and petals are postembryonic organs. To induce callus from petal explants, a higher level of 2,4-D than in the normal CIM was required (see Experimental Procedures). First we looked at shoot apical meristem (SAM) markers, *pWUS::GFP-ER*, *pCLV3::GFP-ER* and *pSTM::STM-VENUS* (Gordon et al., 2007; Heisler et al., 2005; Jonsson et al., 2005; Reddy and Meyerowitz, 2005) in callus derived from aerial organs because their lineages were thought to be closer to SAM than the root meristem. However, SAM markers did not show clear expression in either cotyledon or petal callus (data not shown). We found, instead, that root tissue markers were expressed in both types of callus and the expression pattern was quite similar to that observed in callus of root origin (Figure 3; Figure S2). The J0121 pericycle marker was expressed at the base of every mature callus (Figures 3A–3C). Both *SCR* and *WOX5* QC reporters were broadly expressed in the subepidermal layer of each callus type (Figures 3D–3F, 3G–3I, 3F′, and 3I′). The *SHR* protein fusion reporter showed a QC-like nuclear localization pattern in the subepidermal layer of every callus and stele-like pattern internal to that, although the signal in cotyledon and petal explants was weak. The *GL2* non-hair epidermal reporter was expressed in the outermost layer of each type of callus in a striped pattern (Figures 3J–3L). Therefore, callus derived from aerial organs differentiates as an LRP-like structure, just as does callus derived from roots, which clearly indicates that generic dedifferentiation or simple selective proliferation of cells of particular types are insufficient to explain callus formation.

Callus Derived from Different Organs Is Enriched in Root Tip-Expressed Genes

To further characterize the molecular identity of callus derived from different organs at a genome-wide scale, we analyzed

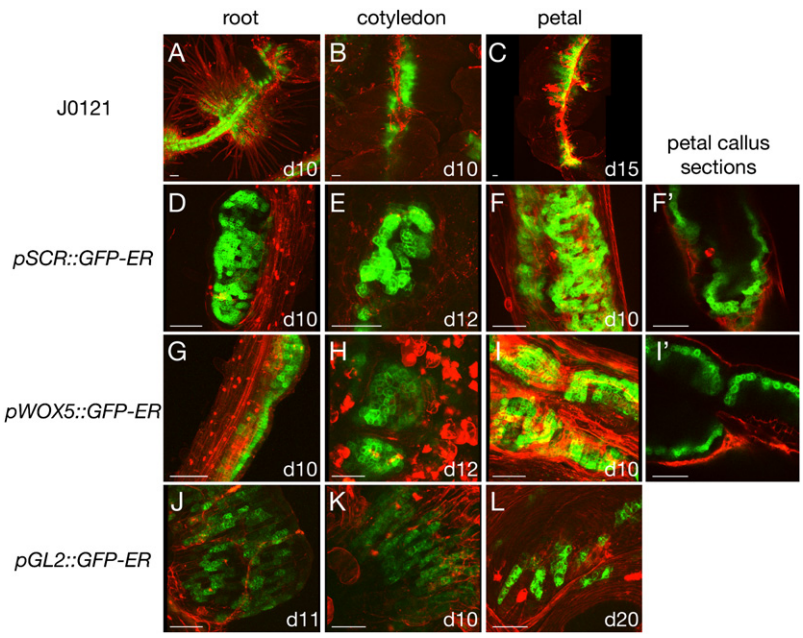

Figure 3. Callus Derived from Aerial Organs Produces Similar Structures to Those of Root Callus

Projections of confocal z-stacks of root tissue marker expression (green) in callus derived from different organs, root (left column), cotyledon (center column), and petal (right column). The number of days of CIM incubation is indicated at the bottom right corner of each panel. Cellular outlines were visualized with propidium iodide staining (red). J0121 (A)–(C), *pSCR::GFP-ER* (D)–(F), *pWOX5::GFP-ER* (G)–(I), and *pGL2::GFP-ER* (J)–(L). (F′, I′) Transverse optical sections of petal callus (F, I). (A)–(C) are basal views of callus. (C) Two sequential projection images are combined. Scale bars represent 50 μm. See also Figure S2.

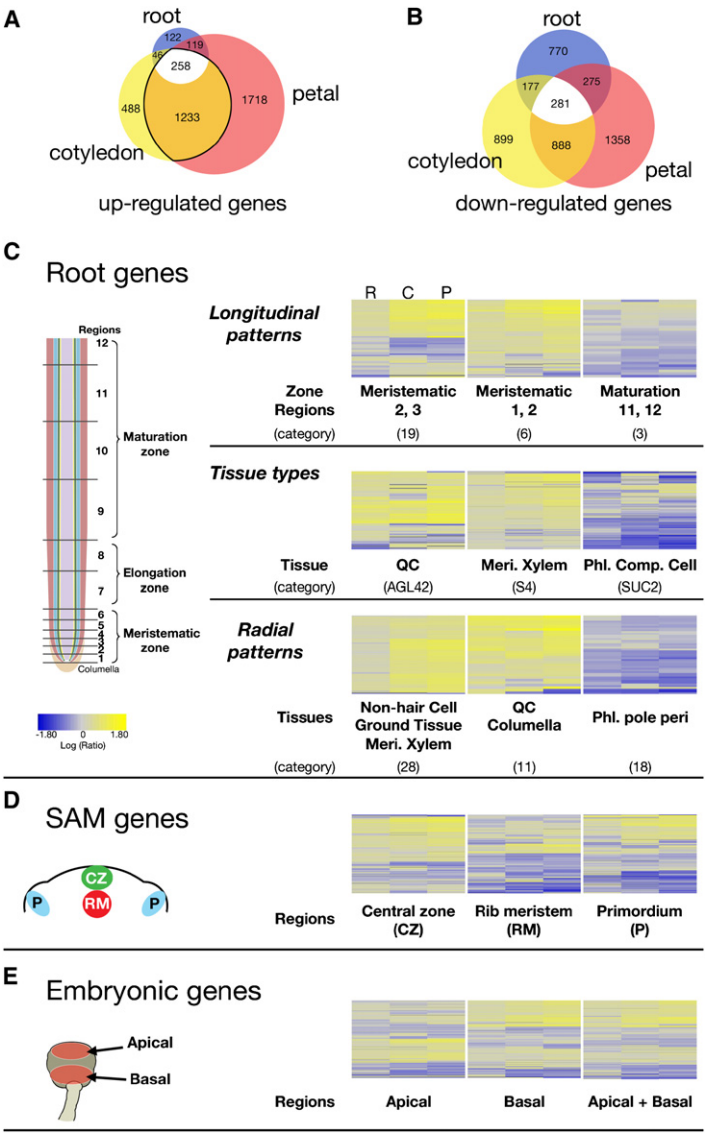

Figure 4. Callus Resembles the Tip Part of the Root Meristem

(A and B) Venn diagrams of the differentially expressed genes that exhibit significant upregulation (A) or downregulation (B) in each callus type compared to its tissue of origin (p value < 0.0001, fold change > 3 or < −3). The black line in (A) surrounds the sector of genes commonly upregulated in cotyledon and petal-derived callus (CP-up genes).

(C) Clustering displays of expression ratios (callus versus its original tissue) for the genes in the top- or bottom-ranked categories. Categories were ranked according to the percentage of CP-up genes included in them (Table S1). All the categories were defined previously based on the specific relative expression pattern of root genes. Meri. Xylem, meristematic zone of xylem; Phl. Comp Cell, phloem companion cells; G Tissue, ground tissue; Phl. pole peri, phloem pole pericycle. The lane order in each cluster is R, C, P (root, cotyledon, petal explants) from the left. Yellow indicates upregulation, and blue indicates downregulation, in callus. Grey indicates that the expression intensity signal was not available (e.g., an absence of signal in one or both of the tissues).

(D and E) Clustering displays of expression ratios for the SAM genes (D) and the globular stage of embryonic genes (E) in each of the three experiments.

See also Figure S3.

transcriptome changes during callus formation via microarrays. The gene expression profile of explants treated with CIM for 10 days was compared to that of their original tissue. The number of upregulated genes in root explants was much smaller than that of cotyledon (26.9%) or petal explants (16.4%) (Figure 4A), suggesting that the callus is more similar to the original tissue in the case of root explants than the other cases. A large portion (47.3% on the basis of total upregulated genes in root) of upregulated genes in the three experiments overlapped, indicating that explants derived from different organs formed tissues with common gene expression patterns. Thus it seems that callus is a root-like tissue regardless of the organ of origin, consistent with the live-imaging data. In contrast to the upregulated genes, the number of downregulated genes in each experiment was similar and the proportional overlap of downregulated gene identities between callus derived from different organs was small (18.7% on the basis of total downregulated genes in root), suggesting that a large proportion of organ-specific genes were downregulated (Figure 4B). For root, only a small portion of root genes (3.1% of expressed genes) were upregulated in callus, while many other root genes were downregulated (8.6% of expressed genes) or unchanged during callus formation. This is again consistent with the live imaging data that indicated that callus represents only the tip part of the root meristem.

To confirm this conclusion and investigate which root tissues are present in callus in more detail, we examined the expression ratios of various sets of root genes previously categorized by their expression pattern (16 tissue types, 46 radial patterns, and 55 longitudinal patterns) (Brady et al., 2007). To determine which categories of root genes are enriched in callus, we used the list of the genes commonly upregulated in cotyledon and petal callus (CP-up genes) from our data (see Figure 4C legend), because the root-specific transcripts abundant in these types of callus should be detected as "upregulated," as the original organs did not express root-specific genes (Figure S3A). We found that callus is enriched in root tip-expressed genes (Figure 4C) (with 27.3%–39.7% of transcripts in the categories found as CP-up genes, $p < 2E\text{-}11$ [Table S1]) but is not enriched in elongation and maturation zone-expressed genes (Figure 4C) (0%–1.6%, $P \approx 1$). Among the tissue type lists, QC cell transcripts (AGL42) were most prevalent in each type of callus (31.5%, $p < 4E\text{-}11$). In addition to this conclusion, we found that genes expressed in the meristematic zone of xylem are abundantly expressed in callus relative to the tissue of origin (18.8%, $p < 1E\text{-}16$), while phloem- and phloem pole pericycle-expressed genes are not (1.4%–2.3%, $P \approx 1$).

Lower but significant transcriptome similarities were also found between callus upregulated genes and certain shoot meristem zones (Yadav et al., 2009) or embryonic tissues (Spencer et al., 2007), which also give rise to new organs in normal plant development. Among SAM domains, callus upregulated genes were enriched in central zone (CZ)-expressed genes (14.4%, $p < 2E\text{-}09$) (Figure 4D; Table S1). Although still significant, CZ

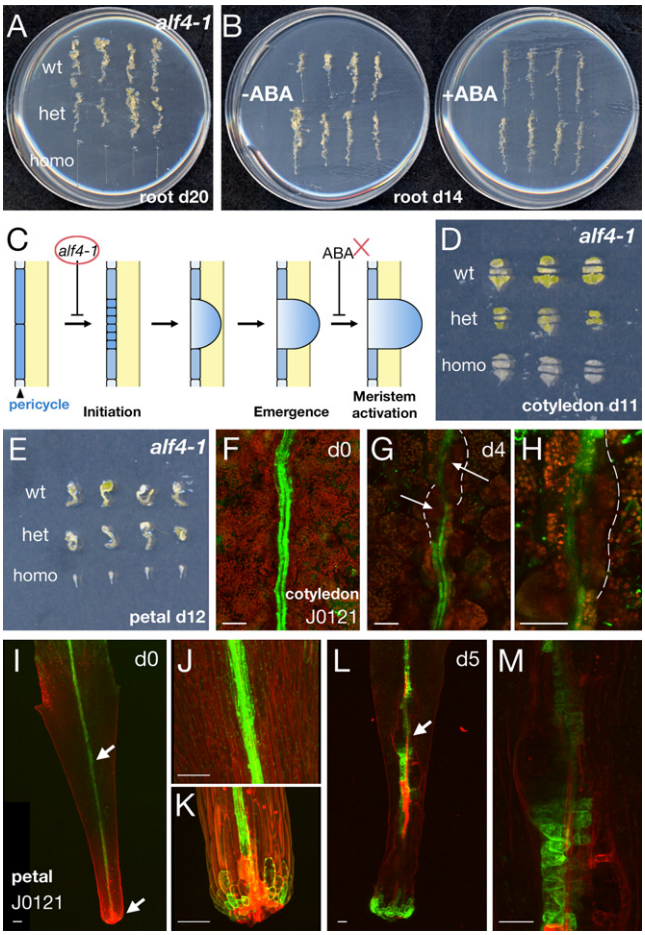

Figure 5. The Link between Callus Formation and Lateral Root Formation

(A) Wild-type and *alf4-1* mutant (heterozygous and homozygous) root explants treated with CIM.

(B) Wild-type root explants incubated on CIM with or without ABA.

(C) Schematic diagram of early lateral root development and the steps the *alf4-1* mutation and ABA inhibit.

(D and E) Wild-type and *alf4-1* mutant cotyledon (D) and petal (E) explants treated with CIM.

(F–H) J0121 reporter expression (green) along the midvein of a cotyledon explant untreated (F) or treated with CIM (G, H). Chlorophyll autofluorescence in red. The arrows in (G) indicate the diffuse appearance of the marker signal. (H) is a magnified view of the part of (G) indicated by the right arrow. White dotted lines in (G, H) indicate growing regions.

(I–M) J0121 reporter expression (green) in the stalk region of petal explant untreated (I–K) or treated with CIM (L, M). Cellular outlines were visualized with propidium iodide staining (red). (J, K) and (M) are magnified views of the parts of (I) and (L) indicated by arrows. The number of days of CIM incubation is indicated at the bottom of (A), (B), (D), and (E) panels, and at the top right corner of (F), (G), (I) and (L) panels.

(I, L, and M) Two or three sequential projection images are combined.

Scale bars represent 50 μm. See also Table S2.

transcripts were proportionally less enriched in CP-up genes than LRP and root tip cell types. More importantly, key genes for SAM development are not expressed in callus (Figure S3B), in contrast to key root meristem development genes (Figure S3A). Instead, we found that many downstream genes, such as cell cycle regulators and metabolic genes, were shared between callus and the CZ. In the globular stage of the embryo, a similarly lower but significant enrichment of the callus upregulated genes was found for basal region genes (13.2%, p = 3E-05) but not apical region genes (8.1%, p = 0.4972) (Figure 4E; Table S1). Because the root meristem is established just after the globular stage, the data showed that callus shares some characteristics with root meristem precursors. Several shoot apex- and seed-specific genes (Becerra et al., 2006; Schmid et al., 2005) are also expressed in callus (Figures S3B and S3C), indicating that callus is not exactly the same as root meristem tissue, but also has traits of additional types of tissues, as assessed by gene expression.

Callus Formation from Root, Cotyledon, and Petal Explants and Lateral Root Formation Are under the Same Genetic Control at the Initial Divisions of Pericycle-like Cells

To validate functionally the conclusion that callus formation resembles lateral root formation and to examine which processes are shared between callus and lateral root formation, we tested the effects on callus formation of mutational or growth conditions that prevent lateral root formation. We chose two conditions that block lateral root development independently of auxin levels, because CIM contains high concentration of 2,4-D. First we examined *alf4* (*aberrant lateral root formation 4*) mutant tissue. *alf4* mutations block initial cell division of pericycle cells, and consequently LRP are rarely formed in *alf4* mutant plants (Celenza et al., 1995). Second, we tested abscisic acid (ABA) treatment, which arrests the outgrowth of LRP just after their emergence (De Smet et al., 2003). Callus formation from root explants was almost completely blocked in *alf4-1* homozygous mutants (3.5%, n = 29) compared to heterozygous and wild-type plants (Figure 5A; Table S2), whereas ABA treatment did not affect callus formation (Figure 5B) although the reported root phenotype of ABA was observed in seedlings grown on medium with the same ABA concentration. Therefore, callus formation probably reproduces the initial developmental program of lateral roots, but does not continue with the program followed after lateral root emergence (Figure 5C). This is direct evidence that the processes involved in pericycle cell division during the formation of lateral roots (Atta et al., 2008; Laplaze et al., 2005) also occur in callus formation.

We examined whether the same developmental program is involved in callus formation from aerial organs that do not produce lateral roots. Callus formation from cotyledons and petals was suppressed in *alf4-1* homozygous mutants (7.7%, n = 39; 0%, n = 41; Figures 5D and 5E; Table S2). ABA-treated petal explants formed callus as normal (data not shown). This result suggests that callus formation and lateral root formation are under the same genetic control at the initiation step, even when the callus derives from aerial organs. However, to date, the term pericycle has been used to describe only a cell layer in the roots of higher vascular plants (Raven et al., 1982). To determine whether there is pericycle-like tissue in aerial organs, we observed the expression of pericycle marker J0121 in cotyledons and petals. The initial strong continuous expression of the marker surrounding the midvein of the cotyledon (Figure 5F) and the petal (Figures 5I–5K) faded at the base of the growing

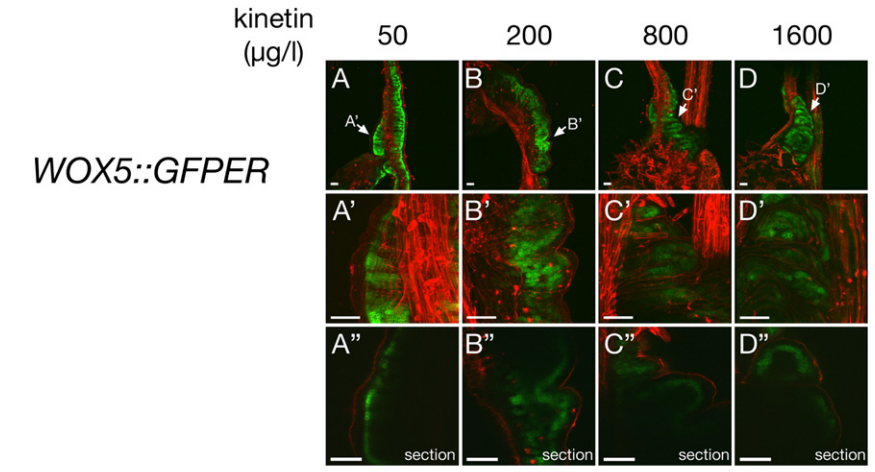

Figure 6. Root-like Callus Is Induced in Various Media Containing Different Ratios of Auxin/Cytokinin

(A–D″) *pWOX5::GFP-ER* expression in root explants treated with CIM containing different concentrations of kinetin: 50, 200, 800, and 1600 μg/l (columns are in this order from the left) for 10 days. All media contain the same concentration of 2,4-D: 500 μg/l. (A′)–(D′) are magnified views of the parts of (A)–(D) indicated by arrows. (A″)–(D″) are single optical sections of (A′)–(D′). Scale bars represent 50 μm.

(E–G) RT-PCR analysis for *18S* ribosomal RNA (loading control) and root meristem-specific gene *WOX5* and *PLT1* expression in root (E), cotyledon (F), and petal (G) explants untreated (d0) or treated with CIM containing different concentration of kinetin (indicated under the bars) for 10 or 11 days (d10 or d11). Concentration of 2,4-D in the medium is 500 μg/l for root and cotyledon, 2000 μg/l for petal.

See also Figure S4.

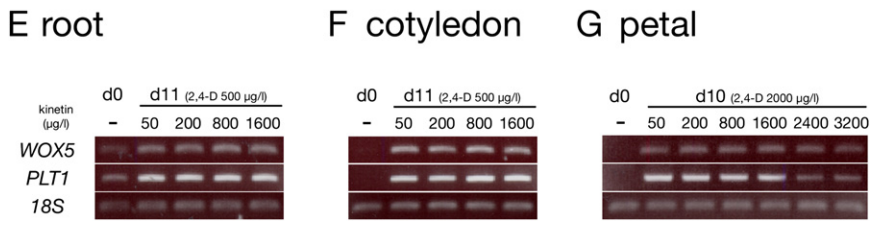

region around the vasculature after the start of CIM treatment (Figures 5G, 5H, 5L, and 5M), similar to what was observed in the initiation of root callus and lateral root (Figures 1B–1D). This suggests that pericycle-like cells are present around the vasculature of multiple organs throughout the plant body and can proliferate and differentiate in response to auxin stimulation.

LRP-like Callus Is Induced in Various Media Containing Different Ratios of Auxin/Cytokinin

Because the type of tissue induced in explants might depend on the auxin-to-cytokinin ratio, we also tested CIM media containing different ratios of auxin/cytokinin than the normal CIM optimized by Valvekens et al. We increased the level of kinetin, a synthetic cytokinin, to make the medium more similar to media that induce shoots (high cytokinin relative to auxin) in callus once it has formed. We found that the *WOX5* reporter is expressed in the subepidermal layer of callus in every medium tested (Figures 6A–6D″), although the signal was weaker and less frequent as the kinetin level increased. Callus formed from root, cotyledon, or petal expressed the root meristem-specific genes *WOX5* and *PLT1* (*PLETHORA1*) in all of the conditions tested (Figures 6E–6G). Therefore, callus in the high-kinetin media resembled root meristem in its patterns of gene expression, just as did callus at a low-kinetin condition in the standard CIM. In addition to this root meritem-like callus, we also found another type of outgrowth in root explants treated with high-cytokinin media, the regeneration capability of which is not known yet (Figure S4). Next, to investigate whether callus formation still occurs via the lateral root initiation program under elevated cytokinin conditions, we assessed the *alf4-1* mutant phenotype with respect to callus formation in the various CIM formulations used above. In *alf4-1* explants, callus formation was strongly reduced in every condition tested (Figure 7), suggesting that callus derivation from pericycle-like cells is under the same genetic control regardless of the medium formulation.

DISCUSSION

In this study, we show that callus formation from multiple organs is not a process of reprogramming to an undifferentiated state, but rather the differentiation of pericycle-like cells present in the organ toward root meristem-like tissue. In this case, the pericyle-like cells are functionally analogous to animal tissue stem cells, which are found in many tissues throughout the body and can divide and differentiate into specialized types of cells. However, the cell types of animal stem cells vary depending on their tissue of origin and are generally limited to differentiating into the original lineage of cell types. It is interesting to note that, in the case of pericycle-like cells, equivalent type of cells exist in different organs and differentiate into common root-meristem-like tissue regardless of the tissue of origin, and regardless of variation in the ratios of hormone concentrations in the medium. Because pericycle has been described as a root tissue, the finding of pericycle-like cells in shoot-derived tissues may give us new insights into plant stem cells. Root pericycle cells at the xylem poles are shown to have meristematic features by their constitutive potency to divide, by morphological characteristics (such as large nuclei, small vacuoles, and dense cytoplasm), and by their shoot-forming capacity (Atta et al., 2008; De Smet et al., 2006; Parizot et al., 2008). How many of these meristematic features are shared between root pericycle cells and pericycle-like cells in other tissues is yet to be examined. Our data suggest a wider developmental potential for pericycle cells as plant stem cells than previously thought.

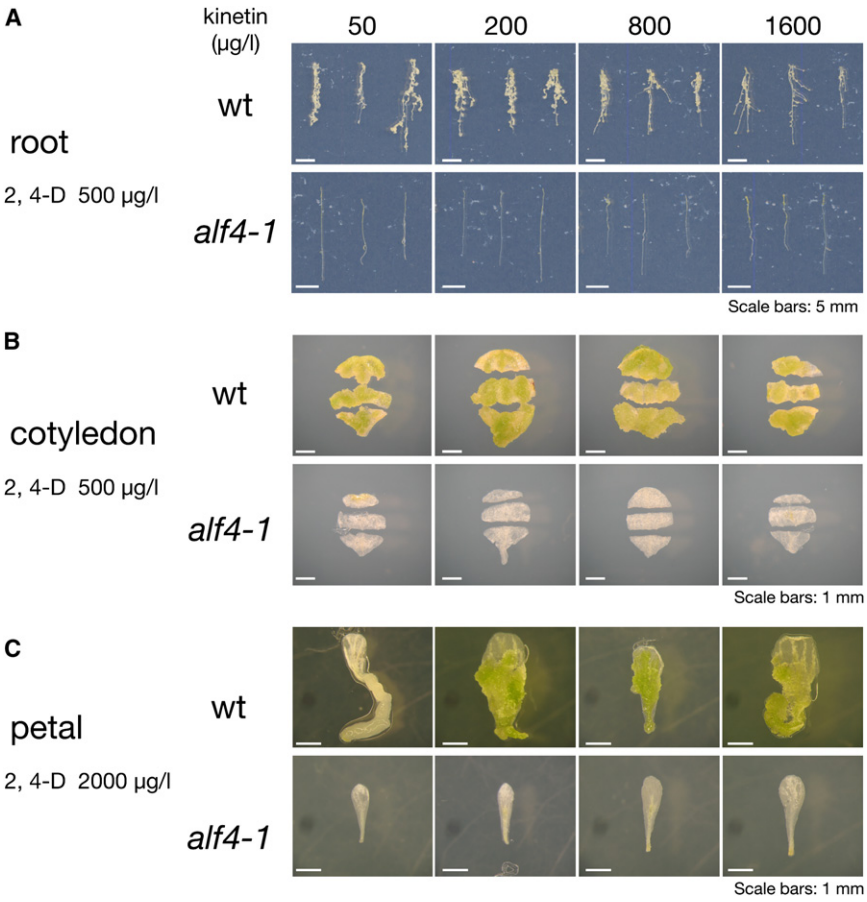

Figure 7. *alf4-1* Blocks Callus Formation in Various Media Containing Different Ratios of Auxin/Cytokinin

Wild-type and *alf4-1* homozygous mutant root (A), cotyledon (B), and petal (C) explants treated for 11 days with CIM containing different concentrations of kinetin. The kinetin concentrations contained in the media are indicated on the panels. The 2,4-D concentrations are 500 μg/l for root and cotyledon media, 2000 μg/l for petal. Scale bars represent 5 mm in (A) and 1 mm in (B) and (C).

Callus-forming cells appear similar to mammalian induced pluripotent stem cells (iPSCs) that are generated by retroviral insertion of several embryonically expressed genes into adult somatic cells, in that various types of somatic tissues can be induced to form a common type of totipotent cell population (Aoi et al., 2008). However, our data show that callus formation is not a process of reprogramming to an embryonic state, like iPS cell generation. This leaves open the question how root meristem-like callus tissue has the ability to form aerial shoots in the next stage of the regeneration process (Gordon et al., 2007). Soon after transfer onto shoot induction medium, gene expression patterns in callus start changing dynamically and shoot genes initiate expression (Banno et al., 2001; Cary et al., 2002). Callus-forming cells are partitioned into regions of different gene expression, and a small number of progenitor cells, found in small patches, initiate development of new shoot meristems (Gordon et al., 2007). Thus, among the shoot-forming explants, there are multiple types of cells, and only limited numbers of cells contribute to new shoot formation. These cells may derive from multiple root-like cell types found in callus, or from only one, in which case one of the root-like cell types found in the callus is itself another type of plant stem cell, much like the pericycle-like cells. These and many other questions remain unanswered. With our new understanding of the nature of callus tissue, they are open for study. Such study will shed light on the mechanisms of plasticity, which occurs in plants to a degree rarely found in animal development.

EXPERIMENTAL PROCEDURES

Plant Materials and Growth Conditions

All of the marker lines used in this study were in the Columbia (Col-0) background (Blilou et al., 2005; Jonsson et al., 2005; Laplaze et al., 2005; Lin and Schiefelbein, 2001; Nakajima et al., 2001; Wysocka-Diller et al., 2000). Plants used for microarray experiments were wild-type plants of Landsberg erecta (Ler). The *alf4-1* mutant alleles have been described before (Celenza et al., 1995; DiDonato et al., 2004). *alf4-1* mutants are male sterile. First-generation progeny seeds from a self-fertilized heterozygous plant were used for experiments and genotyped. Plants were grown on soil or Murashige and Skoog basal salt (MS) medium under continuous light. For ABA treatment, 0.1 mM KNO_3 was added to the basic MS medium with or without 1.0 μM ABA (Sigma).

Regeneration Assays

Root and cotyledon explants were excised from seedlings at 10 days after germination. Cotyledons were cut into three or four pieces. Petal explants were taken from flowers at stages 14 to 15 (Smyth et al., 1990). Explants were cultured on callus-inducing medium (CIM), containing Gamborg's B-5 medium (Sigma) with 20 g/l glucose, 0.5 g/l MES (Sigma), 1× Gamborg's vitamin solution (Sigma), 500 μg/l (for root and cotyledon explants) or 2 mg/l (for petal explants) of 2,4-D (Sigma), and 50 μg/l of kinetin (Sigma). The pH was adjusted to 5.7 using 1.0 M KOH.

To test the effects of different ratios of auxin/cytokinin on callus formation, the concentration of kinetin contained in CIM was changed (50, 200, 800, 1600, 2400, 3200 μg/l), while 2,4-D concentration was fixed (500 μg/l for root and cotyledon explants and 2 mg/l for petal explants).

For ABA treatment, 0.1 mM KNO_3 was added to the basic CIM medium with or without 1.0 μM ABA (Sigma). Mutant analysis and ABA treatment experiments were performed at least three times with different batches of media.

Live Imaging and Microscopy

50 μg/ml of propidium iodide (Sigma) was applied to samples prior to imaging for the counterstaining of cell outlines. All imaging was done with a Zeiss LSM 510 Meta confocal microscope with a 10× objective or a 40× water-dipping lens. To detect the signal of propidium iodide staining, a 488 nm laser line was used for excitation and a 585–615 nm band-pass filter in conjunction with a 545 nm secondary dichroic was used for collection of the signal. For the detection of other fluorescent markers, similar sets of laser and filters were used to those already described (Heisler et al., 2005; Reddy and Meyerowitz, 2005). The Z-stacks were reconstructed into a projection view with Zeiss LSM software. 20 to 30 samples were imaged for each marker line to confirm that observed patterns were representative of the respective markers.

To detect the signal of fluorescent markers in untreated or early stages of cotyledon explants (d0–d6), air bubbles contained in specimen were removed before observation. The samples were mounted on a glass slide with 0.1% of Triton-X (sigma) and were pushed down from the top by a coverslip.

Tissue Collection and Microarray Experiments

Root, cotyledon, and petal explants were collected just after being excised from plants (d0) or after 10 days on CIM (d10). Samples derived from the same organ were cohybridized in the array experiments.

Total RNA was isolated from collected explants with TRIZOL (Invitrogen) and purified with an RNeasy kit (QIAGEN). Purified RNA was assessed for integrity with an Agilent 2100 Bioanalyzer. The methods for amplification of mRNA and labeling of RNA were described previously (Wellmer et al., 2004). Hybridization procedures were described previously (Wellmer et al., 2006).

Each experiment was performed on four independent sets of biological replicates with different batches of medium. The dyes labeling each pair of RNAs were switched in the replicate experiments to reduce dye-related artifacts.

Microarray Data Analysis

Microarrays were scanned with a GenePix 4200A scanner, with the Gene Pix 5.0 software (Axon Instruments). Raw data were imported into the Resolver gene expression data analysis system version 4.0 (Rosetta Biosoftware) and processed as described previously (Wellmer et al., 2006). We adjusted the p values for differential expression calculated with Resolver for each tissue with the Benjamini and Hochberg procedure as implemented in the Bioconductor *multtest* package (http://www.bioconductor.org/packages/bioc/stable/src/contrib/html/multtest.html). A reproducible significant intensity above that of 95% of negative controls in three out of four replicate experiments in at least one channel was used as the threshold to classify a probe as detecting a positive signal of gene expression (Jiao et al., 2008). In all experiments, this empirical expression threshold ensured the detection of >99% of positive controls. Genes were considered as up- or downregulated if they showed an absolute fold-change value more than 3 between d10 and d0 explants and had been assigned an adjusted p value < 0.0001. The intensity data of the replicate experiments were subsequently combined.

The lists of the root genes were from Brady et al. (2007). To determine which categories of root genes are enriched in callus, the number of CP-up genes contained in each category was counted, and then the categories were ranked according to the percentage of CP-up genes included in them (Table S1). Permutation tests were used to assess the statistical significance (p value) of CP-up gene enrichment in each category. In each Monte Carlo simulation, we randomly selected 1491 genes as CP-up genes and the same number of genes as each category from all expressed genes and then calculated the overlapping portion. Across 1,000,000,000 such simulations, the overlapping portions were all distributed in accordance with the Student's t test distribution. A one-sided p value was calculated as the fraction of 1,000,000,000 Monte Carlo simulation values that are at least as extreme as the original statistic observed from experiments. p values less than 1E-09 were computed from the hypergeometric distribution. To control false discovery rate (FDR) for the above enrichment tests, q values were calculated. FDR was assessed at below 5E-04 at our p value cutoff of 1E-04. Hierarchical clustering analysis was done with Rosetta Resolver. Average link was used as the heuristic criterion and Euclidean distance was used as the similarity measure for the sequence cluster algorithm.

The lists of shoot apical meristem (SAM) genes were from Yadav et al. (2009), in which central zone (CZ)-specific genes were categorized as sector 5 defined by *CLAVATA3* expression, rib meristem (RM)-specific genes as sector 6 defined by *WUSCHEL* expression, and primordium (P)-specific genes as sector 7 defined by *FILAMENTOUS FLOWER*. The gene lists of apical and basal parts of the globular stage of embryo were constructed with the data from Spencer et al. (2007). Genes that showed a normalized mean value more than 2.8, or a normalized SD signal value less than 15, were placed on the lists (496 apical genes and 530 basal genes). 912 unique genes from the both lists were put in the list of apical and basal genes. One-sided p values for significance of enrichment were calculated as described above based on 1,000,000,000 Monte Carlo simulations.

RT-PCR

1 μg of total RNA, isolated from explants with an RNeasy kit (QIAGEN), was reverse-transcribed with Superscript II (Invitrogen). 4% of the resulting cDNA was subjected to PCR. The primer sets and cycling condition used for amplification of *18S* were: 18S-fwd (5′-TCAACTTTCGATGGTAGGATAGTG-3′), 18S-rev (5′-CCGTGTCAGGATTGGGTAATTT-3′) and 25 cycles; for *WOX5*: 147644-left (5′-CTGTTTCGAGCCGGTCTTAG-3′), 147644-right (5′-TCACCTTCTCTTCCTCTTGACA-3′) and 30 cycles; for *PLT1*: cPLT1-355L (5′-acgaaaaccaatccaaccac-3′), cPLT1-757R (5′-cctagactggccttcccttc-3′) and 30 cycles (Aida et al., 2004).

ACCESSION NUMBERS

The data are deposited in NCBI GEO under accession number GSE19863.

SUPPLEMENTAL INFORMATION

Supplemental Information includes four figures and two tables and can be found with this article online at doi:10.1016/j.devcel.2010.02.004.

ACKNOWLEDGMENTS

We thank B. Scheres for the *pWOX5::GFPER* seeds, J. Schiefelbein for the *pGL2::GFPER* seeds, P.N. Benfey for the *pSCR::GFPER* and *pSHR::SHR-GFP* seeds, and J.L. Celenza, Jr. for the *alf4-1* seeds. We thank S. Gordon for the help and valuable comments in setting up this project, V. Rao for advice on microarray analysis, A. Garda for technical assistance and advice, and J. Harrison, C. Peterson, and members of Meyerowitz lab for critical reading and comments on the manuscript. We are grateful to A. Roeder for her continuous support and all her suggestions on this project. This research was supported by a Gosney Postdoctoral Fellowship and grant IOS-0846192 from the National Science Foundation.

Received: September 21, 2009
Revised: December 16, 2009
Accepted: February 3, 2010
Published: March 15, 2010

REFERENCES

Aida, M., Beis, D., Heidstra, R., Willemsen, V., Blilou, I., Galinha, C., Nussaume, L., Noh, Y.S., Amasino, R., and Scheres, B. (2004). The PLETHORA genes mediate patterning of the *Arabidopsis* root stem cell niche. Cell *119*, 109–120.

Aoi, T., Yae, K., Nakagawa, M., Ichisaka, T., Okita, K., Takahashi, K., Chiba, T., and Yamanaka, S. (2008). Generation of pluripotent stem cells from adult mouse liver and stomach cells. Science *321*, 699–702.

Atta, R., Laurens, L., Boucheron-Dubuisson, E., Guivarc'h, A., Carnero, E., Giraudat-Pautot, V., Rech, P., and Chriqui, D. (2008). Pluripotency of Arabidopsis xylem pericycle underlies shoot regeneration from root and hypocotyl explants grown in vitro. Plant J. *57*, 626–644.

Banno, H., Ikeda, Y., Niu, Q.W., and Chua, N.H. (2001). Overexpression of *Arabidopsis* ESR1 induces initiation of shoot regeneration. Plant Cell *13*, 2609–2618.

Becerra, C., Puigdomenech, P., and Vicient, C.M. (2006). Computational and experimental analysis identifies *Arabidopsis* genes specifically expressed during early seed development. BMC Genomics *7*, 38.

Birnbaum, K.D., and Sanchez Alvarado, A. (2008). Slicing across kingdoms: regeneration in plants and animals. Cell *132*, 697–710.

Blilou, I., Xu, J., Wildwater, M., Willemsen, V., Paponov, I., Friml, J., Heidstra, R., Aida, M., Palme, K., and Scheres, B. (2005). The PIN auxin efflux facilitator network controls growth and patterning in *Arabidopsis* roots. Nature *433*, 39–44.

Brady, S.M., Orlando, D.A., Lee, J.Y., Wang, J.Y., Koch, J., Dinneny, J.R., Mace, D., Ohler, U., and Benfey, P.N. (2007). A high-resolution root spatiotemporal map reveals dominant expression patterns. Science *318*, 801–806.

Cary, A.J., Che, P., and Howell, S.H. (2002). Developmental events and shoot apical meristem gene expression patterns during shoot development in *Arabidopsis thaliana*. Plant J. *32*, 867–877.

Celenza, J.L., Jr., Grisafi, P.L., and Fink, G.R. (1995). A pathway for lateral root formation in *Arabidopsis thaliana*. Genes Dev. *9*, 2131–2142.

Che, P., Lall, S., and Howell, S.H. (2007). Developmental steps in acquiring competence for shoot development in *Arabidopsis* tissue culture. Planta *226*, 1183–1194.

De Smet, I., Signora, L., Beeckman, T., Inze, D., Foyer, C.H., and Zhang, H. (2003). An abscisic acid-sensitive checkpoint in lateral root development of *Arabidopsis*. Plant J. *33*, 543–555.

De Smet, I., Vanneste, S., Inze, D., and Beeckman, T. (2006). Lateral root initiation or the birth of a new meristem. Plant Mol. Biol. *60*, 871–887.

DiDonato, R.J., Arbuckle, E., Buker, S., Sheets, J., Tobar, J., Totong, R., Grisafi, P., Fink, G.R., and Celenza, J.L. (2004). *Arabidopsis* ALF4 encodes a nuclear-localized protein required for lateral root formation. Plant J. *37*, 340–353.

Gautheret, R.J. (1966). Factors Affecting Differentiation of Plant Tissues Grown In Vitro (Amsterdam: North-Holland).

Geldner, N., Richter, S., Vieten, A., Marquardt, S., Torres-Ruiz, R.A., Mayer, U., and Jurgens, G. (2004). Partial loss-of-function alleles reveal a role for GNOM in auxin transport-related, post-embryonic development of *Arabidopsis*. Development *131*, 389–400.

Gordon, S.P., Heisler, M.G., Reddy, G.V., Ohno, C., Das, P., and Meyerowitz, E.M. (2007). Pattern formation during de novo assembly of the *Arabidopsis* shoot meristem. Development *134*, 3539–3548.

Grieneisen, V.A., Xu, J., Maree, A.F., Hogeweg, P., and Scheres, B. (2007). Auxin transport is sufficient to generate a maximum and gradient guiding root growth. Nature *449*, 1008–1013.

Halperin, W. (1986). Attainment and Retention of Morphogenetic Capacity In Vitro (Orlando: Academic Press).

Heisler, M.G., Ohno, C., Das, P., Sieber, P., Reddy, G.V., Long, J.A., and Meyerowitz, E.M. (2005). Patterns of auxin transport and gene expression during primordium development revealed by live imaging of the *Arabidopsis* inflorescence meristem. Curr. Biol. *15*, 1899–1911.

Jiao, Y., Riechmann, J.L., and Meyerowitz, E.M. (2008). Transcriptome-wide analysis of uncapped mRNAs in *Arabidopsis* reveals regulation of mRNA degradation. Plant Cell *20*, 2571–2585.

Jonsson, H., Heisler, M., Reddy, G.V., Agrawal, V., Gor, V., Shapiro, B.E., Mjolsness, E., and Meyerowitz, E.M. (2005). Modeling the organization of the WUSCHEL expression domain in the shoot apical meristem. Bioinformatics *21* (*Suppl 1*), i232–i240.

Kurup, S., Runions, J., Kohler, U., Laplaze, L., Hodge, S., and Haseloff, J. (2005). Marking cell lineages in living tissues. Plant J. *42*, 444–453.

Laplaze, L., Parizot, B., Baker, A., Ricaud, L., Martiniere, A., Auguy, F., Franche, C., Nussaume, L., Bogusz, D., and Haseloff, J. (2005). GAL4-GFP enhancer trap lines for genetic manipulation of lateral root development in *Arabidopsis thaliana*. J. Exp. Bot. *56*, 2433–2442.

Lin, Y., and Schiefelbein, J. (2001). Embryonic control of epidermal cell patterning in the root and hypocotyl of *Arabidopsis*. Development *128*, 3697–3705.

Malamy, J.E., and Benfey, P.N. (1997). Organization and cell differentiation in lateral roots of *Arabidopsis thaliana*. Development *124*, 33–44.

Nakajima, K., Sena, G., Nawy, T., and Benfey, P.N. (2001). Intercellular movement of the putative transcription factor SHR in root patterning. Nature *413*, 307–311.

Parizot, B., Laplaze, L., Ricaud, L., Boucheron-Dubuisson, E., Bayle, V., Bonke, M., De Smet, I., Poethig, S.R., Helariutta, Y., Haseloff, J., et al. (2008). Diarch symmetry of the vascular bundle in *Arabidopsis* root encompasses the pericycle and is reflected in distich lateral root initiation. Plant Physiol. *146*, 140–148.

Raven, P.H., Evert, R.F., and Curtis, H. (1982). Biology of Plants (New York: Worth Publishers).

Reddy, G.V., and Meyerowitz, E.M. (2005). Stem-cell homeostasis and growth dynamics can be uncoupled in the *Arabidopsis* shoot apex. Science *310*, 663–667.

Sabatini, S., Heidstra, R., Wildwater, M., and Scheres, B. (2003). SCARECROW is involved in positioning the stem cell niche in the *Arabidopsis* root meristem. Genes Dev. *17*, 354–358.

Schmid, M., Davison, T.S., Henz, S.R., Pape, U.J., Demar, M., Vingron, M., Scholkopf, B., Weigel, D., and Lohmann, J.U. (2005). A gene expression map of *Arabidopsis thaliana* development. Nat. Genet. *37*, 501–506.

Skoog, F., and Miller, C.O. (1957). Chemical regulation of growth and organ formation in plant tissues cultured in vitro. Symp. Soc. Exp. Biol. *54*, 118–130.

Smyth, D.R., Bowman, J.L., and Meyerowitz, E.M. (1990). Early flower development in *Arabidopsis*. Plant Cell *2*, 755–767.

Spencer, M.W., Casson, S.A., and Lindsey, K. (2007). Transcriptional profiling of the *Arabidopsis* embryo. Plant Physiol. *143*, 924–940.

Valvekens, D., Montagu, M.V., and Lijsebettens, M.V. (1988). *Agrobacterium tumefaciens*-mediated transformation of *Arabidopsis thaliana* root explants by using kanamycin selection. Proc. Natl. Acad. Sci. USA *85*, 5536–5540.

Vogel, G. (2005). How does a single somatic cell become a whole plant? Science *309*, 86.

Weigel, D., and Glazebrook, J. (2002). Arabidopsis: A Laboratory Manual (New York: Cold Spring Harbor Laboratory Press).

Wellmer, F., Alves-Ferreira, M., Dubois, A., Riechmann, J.L., and Meyerowitz, E.M. (2006). Genome-wide analysis of gene expression during early *Arabidopsis* flower development. PLoS Genet. *2*, e117.

Wellmer, F., Riechmann, J.L., Alves-Ferreira, M., and Meyerowitz, E.M. (2004). Genome-wide analysis of spatial gene expression in *Arabidopsis* flowers. Plant Cell *16*, 1314–1326.

Wysocka-Diller, J.W., Helariutta, Y., Fukaki, H., Malamy, J.E., and Benfey, P.N. (2000). Molecular analysis of SCARECROW function reveals a radial patterning mechanism common to root and shoot. Development *127*, 595–603.

Yadav, R.K., Girke, T., Pasala, S., Xie, M., and Reddy, G.V. (2009). Gene expression map of the *Arabidopsis* shoot apical meristem stem cell niche. Proc. Natl. Acad. Sci. USA *106*, 4941–4946.